



Chemical weathering and atmospheric carbon dioxide (CO₂) consumption in Shanmuganadhi, South India: evidences from groundwater geochemistry

F. Vinnarasi · K. Srinivasamoorthy · K. Saravanan · S. Gopinath ·
R. Prakash · G. Ponnunani · C. Babu

Received: 13 September 2019 / Accepted: 12 February 2020 / Published online: 24 February 2020
© Springer Nature B.V. 2020

Abstract Chemical weathering in a groundwater basin is a key to understanding global climate change for a long-term scale due to its association with carbon sequestration. The present study aims to characterize and to quantify silicate weathering rate (SWR), carbon dioxide consumption rate and carbonate weathering rate (CWR) in hard rock terrain aided by major ion chemistry. The proposed study area Shanmuganadhi is marked with superior rainfall, oscillating temperature and runoff with litho-units encompassing charnockite and hornblende–biotite gneiss. Groundwater samples ($n = 60$) were collected from diverse locations and analysed for major chemical constituents. Groundwater geochemistry seems to be influenced by geochemical reactions combining dissolution and precipitation of solids, cation exchange and adsorption along with minor contribution from anthropogenic activities. The SWR calculated for charnockite and hornblende–biotite gneiss was $3.07 \text{ tons km}^{-2} \text{ year}^{-1}$ and

$5.12 \text{ tons km}^{-2} \text{ year}^{-1}$, respectively. The calculated CWR of charnockite and hornblende–biotite gneiss was $0.079 \text{ tons km}^{-2} \text{ year}^{-1}$ and $0.74 \text{ tons km}^{-2} \text{ year}^{-1}$, respectively. The calculated CO₂ consumption rates via silicate weathering were $1.4 \times 10^3 \text{ mol km}^{-2} \text{ year}^{-1}$ for charnockite and $5.8 \times 10^3 \text{ mol km}^{-2} \text{ year}^{-1}$ for hornblende–biotite gneiss. Lithology, climate and relief were the key factors isolated to control weathering and CO₂ consumption rates.

Keywords Silicate weathering rate (SWR) · Carbonate weathering rate (CWR) · Carbon dioxide consumption · Geochemical reactions · Oscillating temperature · Cation exchange

Introduction

Chemical weathering is a continuous landscape building process which is known to have a profound effect on moderating the global carbon cycle and Earth's climate (Walker et al. 1981a, b; Berner et al. 1983), accounting for nearly half of the consumption of atmospheric carbon dioxide globally (Beaulieu et al. 2012). From hydrogeological point of view, chemical weathering is important because it transforms the solid bedrock into small fragments which constitute aquifers (Talabi 2015). Chemical weathering occurs due to interaction of weak carbonic acid

F. Vinnarasi · K. Srinivasamoorthy (✉) · R. Prakash ·
G. Ponnunani · C. Babu
Hydrogeology Lab, Department of Earth Sciences,
Pondicherry University, Puducherry 605 014, India
e-mail: moorthy_ks@yahoo.com

K. Saravanan
Soil Mechanics Lab, Department of Civil Engineering,
Indian Institute of Science, Bangalore 560012, India

S. Gopinath
Institute of Geophysics, Universidad Nacional Autónoma
de México, Mexico City CP 04510, Mexico

with source rocks, resulting in incongruent or congruent dissolution of rocks forming a new mineral aided by leaching of major ions, trace and rare-earth elements (Pande et al. 1994). It has long been recognized that the dissolution of minerals and chemical weathering act as long-term (> 1 Ma) feedback on the Earth's climate changes (Walker et al. 1981a, b; Berner et al. 1983). Silicate weathering responds rapidly to climate change (< 100 years) and may act as a key component in regulating atmospheric CO_2 level (Beaulieu et al. 2012), since CO_2 is consumed during weathering that significantly alters the climate (Walker et al. 1981a, b). Silicate weathering directs climatic and tectonic forcing via hydrological processes and imposes thermodynamic limit on weathering fluxes, based on physical and chemical properties of water (Maher and Chamberlain 2014). Chemical weathering of silicate minerals is responsible for nearly half of global silicate weathering and accounts for approximately 50–75% of CO_2 consumed on the continents controlled by climatic and geological factors (Berner 1991). It has been recognized that CO_2 flux consumed by carbonate dissolution on the continents is balanced by the CO_2 flux released to atmosphere from oceans by carbonate precipitation; hence, during carbonate weathering there is no net loss of atmospheric CO_2 (Berner et al. 1983).

On geological timescales, the volume of CO_2 in the atmosphere is aided by processes such as organic carbon, carbonate carbon sedimentation and burial, carbonate, organic carbon, silicate weathering on land, volcanic and metamorphic release of CO_2 (Garrels and Mackenzie 1967). Current evidences suggest chemical weathering sensitive to climate change (Tipper et al. 2012). Attempt made by (Gislason et al. 1996) and (Beaulieu et al. 2012) in Mackenzie River basin, north-west Canada, suggests an increase in atmospheric CO_2 due to chemical weathering. The study on chemical and isotopic composition of Indian rivers has been attempted (Sarin et al. 1989). Attempt has also been made to isolate the role of weathering in controlling global riverine fluxes and atmosphere CO_2 drawdown based on whole-rock mineralogy and chemistry (Gaillardet et al. 1999). Approaches utilizing chemistry of water to determine the mobility and fluxes of elements and its control on chemical weathering rates and CO_2 consumption have been attempted (Roy et al. 1999; Gurumurthy et al. 2012). But fewer attempts are made in view of influence of

chemical weathering and uptake of CO_2 in ground-water environment (Calmels et al. 2011). One of the most reliable ways of studying weathering reactions in natural settings is the quantification of the mass fluxes into and out of watershed systems (Donnini et al. 2016).

The aim of the study is to calculate the present-day silicate and carbonate weathering rates using mass balance methods, carbon dioxide consumption and hydrogeochemical functioning of aquifer waters from Shanmuganadhi River basin and to compare the results with global estimations of CO_2 consumption rates. Geologically, the proposed area encompasses two diverse litho-units, charnockite and hornblende–biotite gneiss, with varying temperatures, slopes, runoffs and uneven distributions of precipitation being the dominant factors to contribute for chemical weathering. Previous attempts pertaining to the study area (Aravinthasamy et al. 2019; Karunanidhi et al. 2019) discussed the fluoride occurrences in groundwater, but as per authors' knowledge the proposed study is first of its kind being attempted to focus on chemical weathering and its influence on hard rock aquifers.

Study area description

The area demarcated for the study is the Shanmuganadhi River basin located between north latitudes $10^\circ 11' 34.06''$ N– $10^\circ 40' 52.34''$ N and east longitudes $77^\circ 21' 30.56''$ E– $77^\circ 40' 3.55''$ E with a total river flow of 55.0 km that drains an area of 812.90 km² (Fig. 1). The river originates at northern flank of Sirumalai hills in Dindigul district, Tamil Nadu, traverses further north and joins Amaravathi River at Alangiyam in Tiruppur district, Tamil Nadu. The study area is bounded in the north by flat topography characterized by gentle to moderate slope with an altitude ranging from 248.0 to 446.0 m above mean sea level followed by well-pronounced undulating topography with prominent hills characterized by steep slope varying in altitude between 446.0 and 2477.0 m above mean sea level in south.

Climatic information

The study area is influenced by continental climatic feature characterized by variations in temperature,

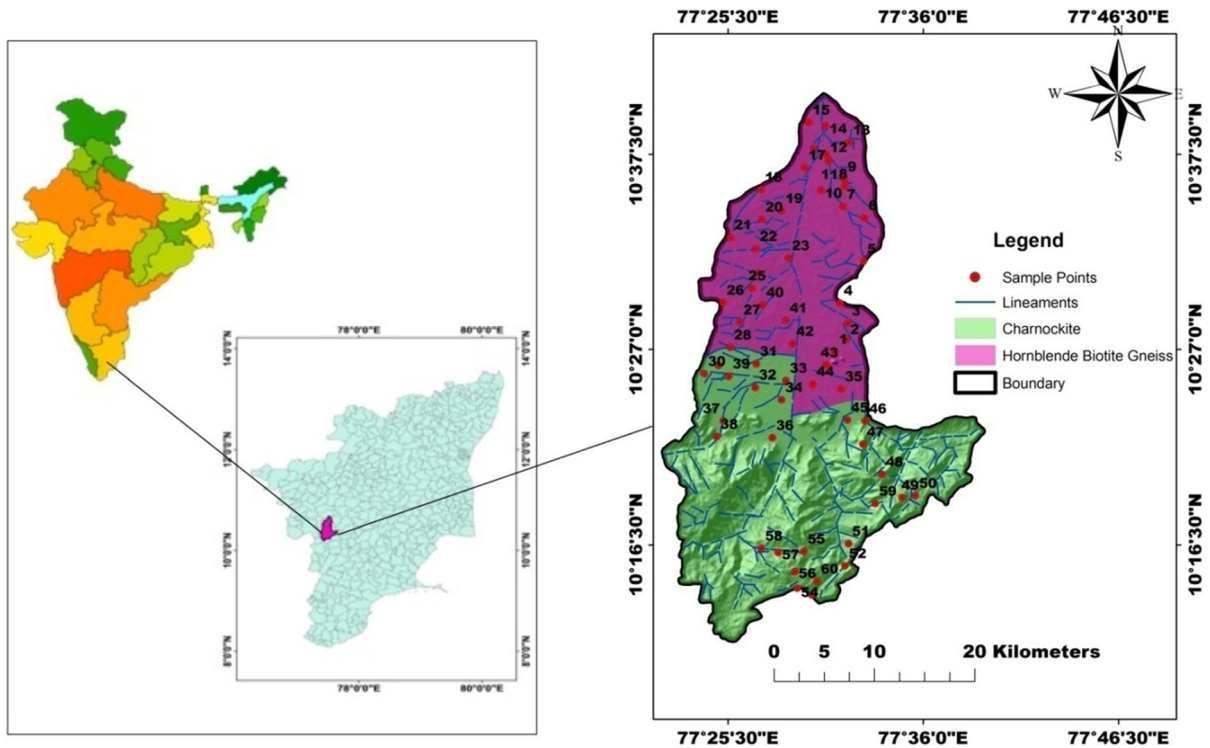


Fig. 1 Location of study area, geology and groundwater sampling points

rainfall and humidity. The area experiences subtropical climatic condition with the average annual rainfall of 700.0 millimetre (mm) to about 1600.0 mm. Scanty rainfall is observed around Palani (709.0 mm) along north-western parts, and a gradual increase in rainfall is observed along south and south-west parts and the rainfall reaches its maximum at Kodaikanal (1606.8 mm) (CGWB 2008). The north-east monsoon which is active during the months of October to December contributes maximum rainfall of about 439.0 mm (50%), followed by south-west monsoon (July to September) 254.0 mm (29.0%), summer (March to June) with 147.0 mm (16.8%) and winter (January to February) of about 26.8 mm (2.8%) (Thangamani and Raviraj 2016). Temperature ranges from a maximum of 37 °C to a minimum of 29 °C during summer and a maximum of 26 °C to a minimum of 20 °C during winter. The relative humidity varies between 65 and 85% in the mornings, and in afternoon, it varies between 40 and 70%. Higher humidity was observed in southern parts of the study area and lower confined to northern parts of the study area.

Geology and hydrogeology

Geologically, the study area falls in Archaean crystalline metamorphic complex with main litho-units encompassing charnockite (CHK) and hornblende–biotite gneiss (HBG) (Fig. 1). Northern portion of the region is entirely composed of HBG (54%), and CHK (46%) is exposed along the southern parts of the study area. Charnockite is formed due to high-grade granulite facies metamorphism of pre-existing igneous rocks, and gneisses are high-grade metamorphic rock in which mineral grains are recrystallized under intense heat and pressure (Sugavanam et al. 1976; Abraham Lerman et al. 2007). Charnockite is a coarse-grained metamorphic rock, dominantly composed of orthopyroxene with enstatite and hypersthene, quartz and K-feldspar minerals. Hornblende–biotite gneiss is a coarse-grained metamorphic rock; its overall dark colouration is due to high levels of mafic mineral hornblende and biotite as alternating layers and other flaky minerals such as feldspar group and quartz.

Groundwater movement in hard rock terrains is mainly through the secondary porosities, viz. fractures, lineament, fissures and cleavages in

unweathered portions and porous zones of weathered formations. Groundwater in the study area occurs in weathered and fractured portions of rocks under semi-confined to confined condition. Groundwater extractions from weathered formation are mainly by dug wells and borewells, and dug cum borewells are used to extract groundwater from fractured formations. The aquifer thickness ranges between 5.2 and 35.4 m for CHK and HBG, respectively. The calculated average groundwater velocities in CHK and HBG were $9.9 \text{ m}^3\text{day}^{-1}$ and $14.3 \text{ m}^3\text{day}^{-1}$, respectively. The calculated average transmissivity values were $8.3 \text{ m}^2\text{day}^{-1}$ and $19.9 \text{ m}^2\text{day}^{-1}$ for CHK and HBG with specific yield of 1.5% irrespective of litho-units (CGWB 2008).

Methodology

Sampling and analytical methods

A total of 60 groundwater samples were collected from CHK and HBG terrains in 60 locations from dug and borewells by considering groundwater flow path, lithology, lineaments and lineament intersection during pre-monsoon period, 2017. Before sampling, the respective wells were purged to remove any stagnant water to provide a representative sample of in situ groundwater with minimum disturbance of the flow system. The samples were filtered using $0.45\text{-}\mu\text{m}$ Millipore filters, and samples were acidified by adding ultrapure nitric acid to pH 2.0 and analysed for chemical constituents. Groundwater chemical analyses were attempted by using standard procedures (APHA 2005). The physical parameters pH, electrical conductivity (EC) and total dissolved solids (TDS) were measured using a multi-probe water analyser. Ions such as Cl^- , HCO_3^- , Ca^{2+} and Mg^{2+} were attempted using titrimetric method, Na^+ and K^+ using ion chromatography and F^- , SO_4^{2-} , PO_4^{3-} , H_4SiO_4 and NO_3^- using an UV spectrophotometer. The data compilation is based on chemical weathering fluxes determined from groundwater chemistry and discharge, adjusted by variable means for atmospheric contribution. The hydrochemical evolution of groundwater is complex, and understanding the process responsible for the evolution is attempted by using geochemical software (PHREEQC 2.1). Major cations

and anions are fed into the model platform, and the model is run with variable pHs and temperatures to calculate the saturation index (SI) of the groundwater samples. The spatial analysis for mapping groundwater chemical evolution was attempted using Arc GIS version 9.3 and interpolated using inverse distance-weighted (IDW) raster technique (Srinivas et al. 2013; Ball et al. 1987).

Results and discussion

Physico-chemical parameters

The geochemistry of groundwater is influenced by factors such as rock type, voids between minerals, secondary fractures, residence time, earlier composition of existing groundwater and other characteristics along the flow path (Toth 1999). The groundwater chemical composition is usually constant with time, and it may vary slightly from well to well due to slow movement and longer residing time as compared to surface water (Corbett 1979). A study of major ions in groundwater of the study area will provide information about the hydrochemical status of aquifer systems. The statistical parameters such as minimum, maximum and average of physico-chemical parameters are listed in Table 1 for both CHK and HBG separately. The median temperature of the groundwater samples is 25°C , which is consistent with the ambient surface temperature of the catchment region.

Physical parameters

The pH of groundwater is an important indicator of its quality, controlled by total dissolved CO_2 (Ghandour et al. 1985). The combination of CO_2 with water forms carbonic acid (H_2CO_3), which affects the pH of the water. The pH in groundwater collected from CHK and HBG terrain indicates alkaline groundwater signifying weathering dominance irrespective of litho-units (Mattson 2014). HBG dominating in EC values $7220.0 \mu\text{S cm}^{-1}$ might be due to higher rate of chemical weathering and dissolution of solutes. Total dissolved solids (TDS) represent the dissolved mineral constituents as the sum of total cations, anions and other elements dissolved in water (Nakagawa et al. 2016). In comparison with CHK, groundwater samples collected in HBG are recorded with higher TDS

Table 1 Statistical values of CHK and HBG during PRM

Parameters	CHK			HBG		
	Min	Max	Avg	Min	Max	Avg
pH	6.0	8.21	7.28	6.91	8.29	7.66
EC	27.0	3860.0	451.7	380.0	7220.0	1996.4
TDS	14.9	2250.0	264.1	221.0	4190.0	1157.9
Ca ²⁺	1.0	65.0	15.5	12.0	260.0	75.8
Mg ²⁺	0.65	92.0	10.0	9.7	210.0	41.3
Na ⁺	2.0	410.0	39.9	22.0	720.0	209.8
K ⁺	0.1	95.0	11.0	8.69	175.0	47.4
NH ₄ ⁺	0.1	7.2	1.8	1.6	35.7	5.7
PO ₄	0.03	1.7	0.60	0.05	11.4	1.0
SO ₄ ²⁻	0.9	100.19	12.7	4.81	244.3	84.2
F ⁻	0.1	1.98	0.3	0.05	2.4	1.4
Cl ⁻	1.75	510.0	56.1	58.0	575.0	297.0
NO ₃ ⁻	0.1	24.0	1.1	0.0197	47.2	9.81
HCO ₃ ⁻	6.0	265.0	46.6	25.0	658.0	216.5
H ₄ SiO ₄	1.9	39.2	20.2	10.9	47.2	29.5

All values in mg L⁻¹ except pH, EC in μS cm⁻¹
Max maximum, *Min* minimum, *Avg* average

(4190.0 mg L⁻¹), inferring longer rock–water interaction and evapotranspiration activities (Olobaniyi et al. 2007; Calmels et al. 2011; Duraisamy et al. 2018). Due to the CHK exposure confined to higher altitudes signifying recently recharge water with lower TDS.

Chemical parameters

The major cations in groundwater are calcium, magnesium, sodium, potassium and ammonia; anions include chloride, fluoride, bromide, nitrate, bicarbonate, phosphate and sulphate. The variation in these ionic concentrations largely depends on host rock of the aquifer, land use, recharge groundwater abstraction pattern, etc. Irrespective of the lithology, the dominance of cations follows the order Na⁺ > Ca²⁺ > Mg²⁺ > K⁺ > NH₄⁺ and for anions in CHK the order of the ionic dominance is as Cl⁻ > HCO₃⁻ > CO₃²⁻ > SO₄²⁻ > NO₃⁻ > PO₄³⁻ > F⁻ > Br⁻ and in HBG F⁻ preceded PO₄³⁻.

Cations Calcium is observed higher in HBG (260.0 mg L⁻¹) in comparison with CHK (65.0 mg L⁻¹), which might be due to dominance of calcium in HBG derived from the chemical weathering of minerals such as Ca-rich plagioclase feldspar (anorthite) and hornblende. Maximum Ca²⁺ in HBG also infers the entry of these ions into the aquatic

solution through more liberation of Ca²⁺ ions from silicate minerals (Nakagawa et al. 2016) from aquifer matrixes. Lower calcium in CHK might be due to the lower availability of calcium-bearing minerals (Ronald Frost and Carol Frost 2008). Magnesium, an alkaline earth metal with 2⁺ oxidation state, is a major constituent of dark-coloured ferromagnesian minerals, particularly olivine, pyroxene, amphiboles and micas. Magnesium is found to be higher (210.0 mg L⁻¹) in groundwater samples from CHK, which might be due to the abundance of magnesium-bearing minerals such as orthopyroxene encompassing enstatite and hypersthene. Sodium and potassium are highly soluble chemical elements which occur naturally in groundwater. Higher Na⁺ (720.0 mg L⁻¹) in groundwater samples from HBG might be due to dissolution of sodium-bearing minerals such as plagioclase group and amphibole group like hornblende that might have contributed sodium (Safei et al. 2015). Potassium is obtained by the dissolution of silicate-bearing minerals such as alkali feldspar, biotite, muscovite and amphiboles from the host rocks (Plummer et al. 2004). During silicate weathering, potassium-bearing feldspar group, i.e. K-feldspar, might release K⁺ ions (Brookins 1988). Higher potassium in HBG (175.0 mg L⁻¹) might be due to releasing from potassium-bearing minerals such as orthoclase and microcline that alter into clay minerals such as

kaolinite and illite which release K^+ ions into the groundwater environment (Peter Ardito 1983).

Anions Sources for ammonia in groundwater are mainly due to anthropogenic activities such as fertilizer leaching, organic waste disposal and leaky sewage systems (Böhlke et al. 2006). Higher ammonia in HBG (35.7 mg L^{-1}) might be due to vegetation and agricultural activities confined along the northern parts of the study area. Phosphate is added to soil by chemical fertilizers, manure and composted materials from agricultural activities (Fuller 1951). Higher phosphate in HBG (11.4 mg L^{-1}) might be due to effective leaching of phosphate minerals from agricultural fields (Guilbert and Dejoy 1979). Sulphate in groundwater can be derived from dissolution/weathering of sulphate including evaporite minerals such as gypsum and anhydrite (CaSO_4). Sulphate is higher in HBG (244.31 mg L^{-1}), indicating greater dissolution of sulphate-bearing minerals and/or leachable sulphate in fertilizer that gets released into the groundwater due to agricultural and human influences. Nitrates in groundwater are mainly natural and anthropogenic sources (Srinivasamoorthy et al. 2008). Higher nitrates observed in HBG (47.2 mg L^{-1}) might be due to intense agricultural activities (Saravanan et al. 2016) confined along the northern parts of the study area. Fluoride in ground water can be both beneficial and dangerous depending on its concentration (Wang et al. 2004). Fluoride enrichment in groundwater might be primarily due to leaching and weathering of the fluoride-bearing minerals such as biotite and hornblende isolated from the litho-units of the study area (Saravanan et al. 2016). Chloride is an important groundwater contaminant mainly from sewage and industrial wastes (Basavarajappa and Manjunatha 2015) and from sources such as dissolution of halite and related minerals (Basavarajappa and Manjunatha 2015). Chloride behaviour in groundwater is considered as conservative, which implies its circulation through hydrological cycle, controlled by physical rather than by chemical process. Chloride is slightly higher in HBG (575.0 mg L^{-1}) than in CHK (510.0 mg L^{-1}), which might be due to the irrigation return flow and rainfall recharge (Hem 1985). Alkalinity indicates the ability for groundwater to neutralize the inputs of acidity, and generally consists of bicarbonate (HCO_3^-). Predominance of HCO_3^- in HBG (658.0 mg L^{-1}) might be due to intense chemical

weathering processes in aquifers and contribution also from natural processes such as incongruent dissolution of silicates in the groundwater that reacts with carbon dioxide might release bicarbonates (Srinivasamoorthy et al. 2012). Silica in groundwater is originated from rock sources, since the process is irreversible; silica retains in aquatic solution, influenced by thermodynamic factors in the dissolution process, and adsorption of silicate minerals (Huang et al. 2015). Higher silica in HBG (47.2 mg L^{-1}) groundwater indicates prolonged interaction between the aquifer rock and water and also the excess release from silicate minerals such as feldspar group, amphibole group and mica group minerals from the host rocks (Stumm and Morgan 1996).

Graphical representation of hydrochemical data

The geological formations, water–rock interaction and relative mobility of ions are the prime factors influencing the geochemistry of the groundwater (Yousef et al. 2009). The graphical representation of hydrochemical data gives quick processing and interpretation of data sets along with detecting the mixing of different water compositions and isolating chemical processes that occur as water flows through the aquifer system. There are several graphical techniques that have been developed for the presentation of chemical components of water. Piper and ionic ratio plots were attempted to discuss the water–rock interaction and aided geochemical interactions in the study area.

Hydrochemical facies of groundwater

The geochemical nature of groundwater can be easily understood by plotting cations and anions in trilinear plot (Piper 1944) which helps in understanding the chemical characteristics of groundwater samples (Fig. 2). The diamond plot is divided into six facies in order to distinguish different types of groundwater. Irrespective of litho-units, 50% of sample falls in mixed $\text{Ca}^{2+}\text{Mg}^{2+}\text{Cl}^-$ and 44% in $\text{Na}^+ - \text{Cl}^-$ type with minor representations: 3% in $\text{Ca}^{2+} - \text{HCO}_3^-$ and 3% in $\text{Ca}^{2+}\text{Na}^+ \text{HCO}_3^- +$ type. Mixed $\text{Ca}^{2+}\text{Mg}^{2+}\text{Cl}^-$ facies indicates prolonged water–rock interaction and matured water types, and mixed $\text{Ca}^{2+}\text{Na}^+\text{HCO}_3^-$ water types suggest mineral dissolution

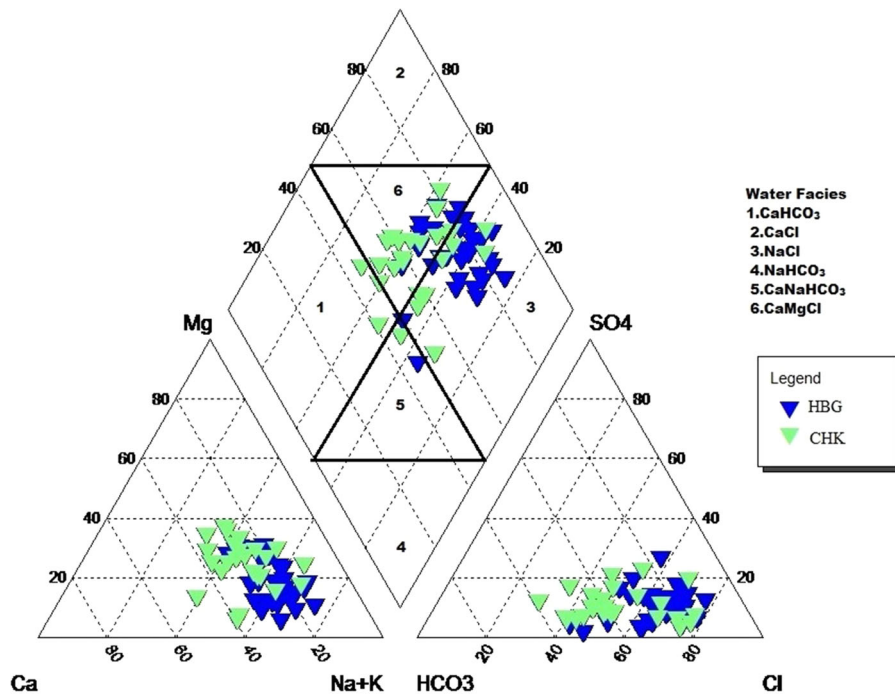


Fig. 2 Piper plot for groundwater samples in view of diverse litho-units (HBG—hornblende–biotite gneiss, CHK—chamockite)

(Srinivasamoorthy et al. 2014). $Ca^{2+} - HCO_3^-$ type water indicates recently recharged water enriched with HCO_3^- and Ca^{2+} . Dissolution of carbonate-bearing minerals, domestic waste water and ion exchange is an important geochemical process for the $Na^+ Cl^-$ type of groundwater. The groundwater geochemical facies generally observed were mixed and $Na^+ Cl^-$ facies indicate prolonged water–rock interaction and matured stage of groundwater environment (Saranvanan et al. 2016).

Ratio diagrams

Weathering of rocks is one among the significant processes that control the geochemical cycling in the aquifer systems (Berg 1932). The nature and rate of chemical weathering differ significantly depending on the interlinked variables together with bedrock type, topography and climatic system. Ionic relationships of various cations versus anions have been plotted to assess their sources (common or varied) to understand the present chemical composition of groundwater (Hounslow 1995). In hard rock terrain, silicate weathering is one of the important geochemical processes which control the major ion chemistry

of groundwater (Garrels and Mackenzie 1967). It is more difficult to quantify silicate weathering products since degradation of silicates minerals due to incongruent nature, which forms a variety of solid phases (mostly clays) along with some dissolved species (Das and Kaur 2001). The impact of silicate and carbonate weathering in regulating the major ion composition is discussed for which the concentrations of the various constituents are converted into $meq L^{-1}$ to combine various ions for meaningful interpretation.

$$Ca^{2+} + Mg^{2+} \text{ versus } HCO_3^- + SO_4^{2-}$$

In the plot of $(Ca^{2+} + Mg^{2+})$ versus $(HCO_3^- + SO_4^{2-})$, samples representing above the equiline suggest carbonate weathering influencing water chemistry and samples representing below the equiline indicate the supremacy of silicate weathering (Datta and Tyagi 1996). The plot (Fig. 3a) suggests the majority of samples confined below the equiline with few exceptions also above, indicating the dominance of silicate weathering in comparison with carbonate weathering irrespective of litho-units.

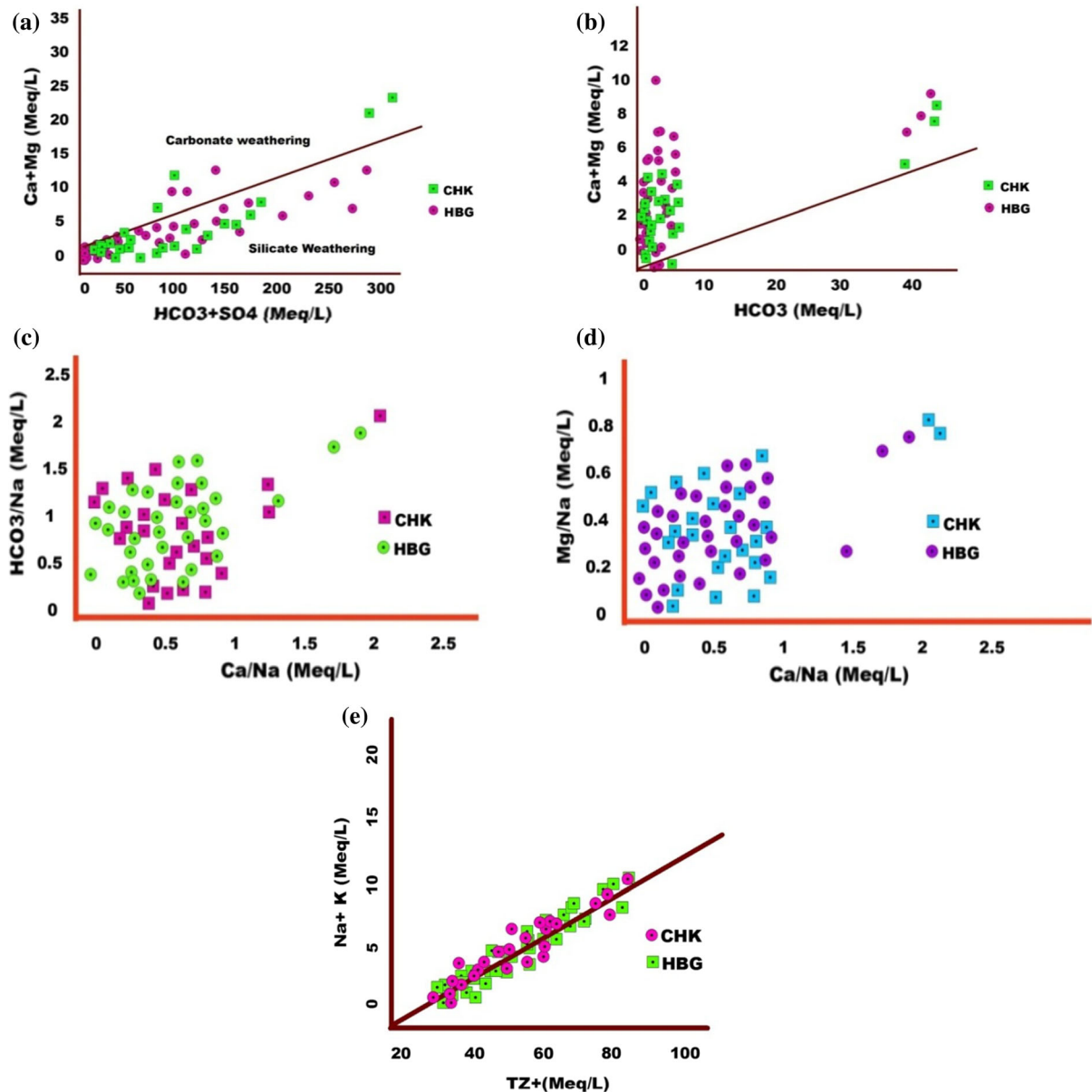


Fig. 3 The ionic ratio plots for **a** $Ca^{2+} + Mg^{2+}$ versus $HCO_3^- + SO_4^{2-}$, **b** $Ca^{2+} + Mg^{2+}$ versus HCO_3^- , **c** HCO_3^-/Na^+ versus Ca^{2+}/Na^+ , **d** Mg^{2+}/Na^+ versus Ca^{2+}/Na^+ , **e** $Na^+ + K^+$ versus TZ^+

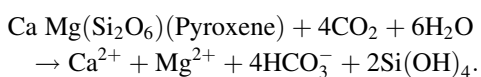
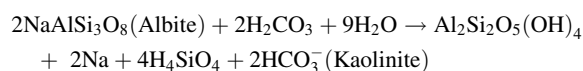
$Ca^{2+} + Mg^{2+}$ versus HCO_3^-

Evidences for silicate weathering can be explained by $Ca^{2+} + Mg^{2+}$ versus HCO_3^- relationship. The plot $Ca^{2+} + Mg^{2+}$ versus HCO_3^- is used to identify ion exchange and weathering processes dominating water chemistry. The plot (Fig. 3b) irrespective of litho-units signifies samples representing above 1:1 equi-line, indicating predominance of alkali earth over

bicarbonate due to silicate weathering, which confirms the significant role of silicate weathering as a primary mechanism in delineating the dissolved ion occurrence in groundwater environment. Minor representations are also observed in bicarbonate zone due to reaction of feldspar minerals with carbonic acid in the presence of water that releases HCO_3^- (Elango et al. 2003; Das et al. 2005).

Silicate weathering

The dissolution of silicate/carbonate minerals might also be sources for increasing sodium and potassium ions in groundwater. Silicate/carbonate weathering as sources for Na⁺ and K⁺ ions can be isolated from HCO₃⁻/Na⁺ versus Ca²⁺/Na⁺ (Fig. 3c) and Mg²⁺/Na⁺ versus Ca²⁺/Na⁺ (Fig. 3d) plots. The plots suggest weathering of silicate minerals as the dominant process influencing groundwater geochemistry by notable increase of Na⁺ than Ca²⁺, Mg²⁺ and HCO₃⁻. Due to higher solubility of Na⁺ relative to Ca²⁺, lower Ca²⁺/Na⁺ ratio is observed in groundwater related to silicate weathering (Rahman et al. 2011). The ratio plot TZ⁺ versus Na⁺+K⁺ is used as an index to assess the contribution of cations by silicate weathering. The plot for Na⁺+K⁺ versus TZ⁺ indicates weathering of both alkali and alkali earth from feldspars along with additional sources from alkali/saline soil and groundwater residence time (Srinivasamoorthy et al. 2009). The samples in the plot (Fig. 3e), irrespective of litho-units, represent along and above the equiline, suggesting cations in groundwater might have been derived from silicate weathering (Lakshmanan et al. 2003). The plot also suggests contribution of sodium and potassium to groundwater due to silicate weathering. Weathering of sodic (albite) and potash feldspars that are common minerals observed in both litho-units of the study area might have contributed Na⁺ and K⁺ ions to the groundwater. Feldspars are more susceptible to weathering and alteration than quartz in silicate rocks (Glover et al. 2012). Silicate dissolution might be the probable source for Na⁺ in the study region, since groundwater primarily derives solutes due to silicate weathering that essentially contain HCO₃⁻ as the most abundant anion (Fisher and Mullican 1997). This is mainly due to the reaction of feldspar minerals with carbonic acid in the presence of water, which releases HCO₃⁻ (Elango et al. 2003), which is illustrated by the following equation:



The primary silicate minerals, such as plagioclase and pyroxene, might be dissolved and weathered to kaolinite, silica and cations such as Na⁺, Ca²⁺ and Mg²⁺ (Guo et al. 2002). Higher HCO₃⁻ clearly indicates the intense chemical weathering processes activated in the study region. From the ratio plot, it is inferred that major cations and HCO₃⁻ sources in the study area are due to weathering of silicates. The contribution of Ca and Mg to groundwater is also due to weathering of silicate-rich minerals such as plagioclase feldspar and pyroxenes which are noted as common minerals in CHK and HBG from the study area.

Saturation indices (SIs) of minerals in groundwater chemistry

The saturation index (SI) approach is to predict the reactive mineralogy of distinct litho-units aided with groundwater chemistry deprived of collecting rock samples and analysing its mineral constituents (Parkhurst et al. 1980). For the present study, geochemical software PHREEQC (Parkhurst et al. 1982) has been used to calculate SI of minerals. The SI is calculated by comparing chemical activities of dissolved ions in view of minerals (ion activity product, IAP) with their solubility product (K_{sp}).

$$\text{SI} = \log(\text{IAP}/K_{\text{sp}}).$$

SI greater than zero indicates mineral precipitated in water (over-saturated), SI less than zero indicates mineral dissolved in water (under-saturated) and SI equal to zero indicates equilibrium state of mineral constituents. The SI of silicate mineral phases such as quartz, chrysotile and chalcedony was observed. Quartz and chalcedony reveal precipitation, and chrysotile shows dissolution along the groundwater flow path (Fig. 4a). The over-saturation of silica mineral species obviously indicates existing of silicate mineral in aquifer matrix. Since the study area is essentially composed of silicate minerals, the rock-water interaction effectively controls the addition of dissolved silica mineral species in groundwater. The over-saturated mineral phases such as quartz and chalcedony signify excess availability of minerals besides prolonged interaction in the groundwater environment. Under-saturated mineral species of chrysotile shows limited avail aquifer mineral

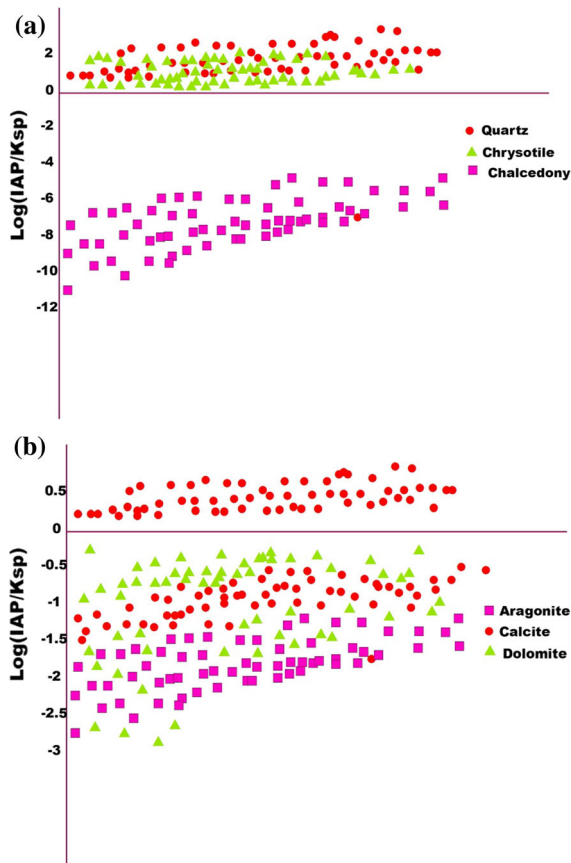


Fig. 4 **a** Saturation indices of groundwater samples with respect to silicate minerals (quartz, chrysotile, chalcedony), **b** saturation indices of groundwater samples with respect to carbonate minerals (aragonite, calcite, dolomite)

matrixes. Carbonate minerals such as aragonite, calcite and dolomite show dissolution along the flow path (Fig. 4b). In CHK and HBG terrains, silicate minerals show precipitation trend and carbonate minerals reveal dissolution. Geochemical weathering causes precipitation and dissolution tendency in HBG and CHK minerals (Srinivasamoorthy et al. 2008).

Sources of major ions

For the estimation of chemical weathering rate, contribution of major ions via atmospheric contribution, chemical weathering and anthropogenic sources has to be considered (Stallard and Edmond 1987). The dissolved concentrations of major ions and their ratios

are examined with suitable assumptions to constrain contributions from these sources.

Atmospheric contribution to groundwater chemistry

Atmospheric deposition of solutes can contribute a significant amount of cations and anions to groundwater. As a result, accurate estimates of the total flux of solutes from the weathering of silicate rocks require correction for atmospheric contributions. The atmospheric contribution to groundwater is mainly from sea salt and atmospheric dust which can be estimated from precipitation water chemistry. Attempt has also been made to collect rainwater samples from the study area and analysed for major ions. Dissolved ions such as Ca^{2+} , Mg^{2+} , Na^+ , K^+ and Cl^- expressed in (micromole/L) were corrected for the atmospheric contributions using the formula suggested by Das et al. (2005)

$$X^* = (X_{\text{GW}} - (X_{\text{RW}}/\text{Cl}_{\text{RW}}) \times (\text{Cl}_{\text{RW}}/\text{ET})) \quad (1)$$

where X^* includes ions Ca^{2+} , Mg^{2+} , Na^+ and K^+ resulting from chemical weathering from the study area; X_{GW} is the micromolar concentration of Ca, Mg, Na and K ions in groundwater; and X_{RW} and Cl_{RW} are the micromolar concentration of ions in rainwater. Evapotranspiration (ET) factor is the most significant component of the hydrological budget calculated by adopting method (Hargreaves and Allen 2003; Karunanidhi et al. 2013). The ET values for CHK and HBG calculated were found to be 2.6 mm day^{-1} and 4.0 mm day^{-1} , respectively. Major ions such as Ca^{2+*} , Mg^{2+*} , Na^{+*} and K^{+*} corrected for atmospheric contributions were used to quantify their weathering rate from different sources into the groundwater.

Anthropogenic input

Irrespective of chemical weathering, pollution due to manmade and anthropogenic activities influences the ionic concentrations in groundwater. The products of anthropogenic activities could enter the subsurface water through agricultural activities and industrial wastewater (Wu et al. 2015). In the groundwater samples, Cl^- and SO_4^{2-} are usually related to human activities; therefore, these ions have been used as

tracer in identifying the degree of anthropogenic contribution (Liu et al. 2018). The influence of anthropogenic activities on groundwater generally termed as pollution index is used to demarcate the zones influenced by contamination (Soumya et al. 2011). (Pacheco and Van der Weijden 1996) defined pollution influence on groundwater using ratio percentages of certain ions such as Cl^- , SO_4^{2-} and HCO_3^- as considering their presence in groundwater due to anthropogenic activities. The pollution index of an area can be calculated by using the formula

$$\begin{aligned} \% \text{Pollution} &= \left\{ (\text{Cl}^- + \text{SO}_4^{2-}) / (\text{Cl}^- + \text{SO}_4^{2-} + \text{HCO}_3^-) \right\} * 100 \end{aligned} \tag{2}$$

where all the concentrations are in $\mu \text{eq L}^{-1}$.

The pollution percentage ≤ 40 in groundwater is considered as a limit of chemical weathering, between 40 and 60% indicates moderate pollution and $> 60\%$ indicates highly polluted (Pacheco and van der Weijden 1996). Percentage of pollution was calculated for groundwater samples and plotted with Na/Cl versus pollution% as shown in Fig. 5. Majority of samples represent within the limit of chemical weathering, suggesting the absence of anthropogenic input with minor representations also in moderate pollution signifying the absence of pollution sources in the study area.

Estimation of silicate weathering rate (SWR) and carbonate weathering rate (CWR)

Major ions such as Ca^{2+*} , Mg^{2+*} , Na^{+*} and K^{+*} corrected for atmospheric and anthropogenic input

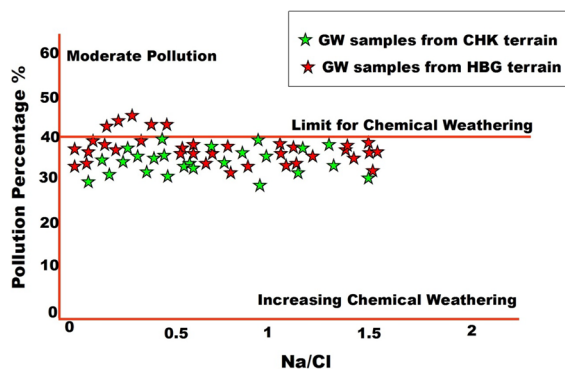


Fig. 5 Sodium/chloride versus pollution %

were used to estimate the chemical weathering rate. Here, “*” indicates ions corrected after atmospheric corrections. Mass balance (MB) approach to estimate the chemical weathering rates has been attempted for the study area. MB is used to quantitatively investigate elemental mobility and rates of elemental transfers in natural hydrogeochemical systems (Clayton 1988). Mass balance is attempted by considering hydrological, precipitation and groundwater chemistry (Katz et al. 1985).

The silicate weathering rate (SWR) $\text{tons km}^{-2} \text{year}^{-1}$ is calculated separately for both CHK and HBG litho-units based on the following relationship (Roy et al. 1999)

$$\begin{aligned} \text{SWR} &= (\text{Na}_{\text{sil}}^+ + \text{K}_{\text{sil}}^+ + \text{Ca}_{\text{sil}}^{2+} + \text{Mg}_{\text{sil}}^{2+} + \text{SiO}_2) \\ &\quad * Q/A / \text{density of silicate} \end{aligned} \tag{3}$$

where Q is the discharge in $\text{m}^3 \text{S}^{-1}$, A is the total surface area in km^2 and Na_{sil} , K_{sil} , Ca_{sil} and Mg_{sil} represent the cations supplied by silicates in mg L^{-1} (Krishnaswami et al. 2005). The calculated discharge values were $3613.5 \text{ m}^3 \text{ year}^{-1}$ and $5219.5 \text{ m}^3 \text{ year}^{-1}$ and the total surface areas considered were 368.318 km^2 and 444.5846 km^2 for both CHK and HBG, respectively. The average density of silicates considered for the present study is 2700 kg m^{-3} as proposed by Galy and France-Lanord (1999). To derive silicate weathering rates, it is necessary to extract the contributions of cations and silica from silicates to the measured major ion composition of groundwater. The estimation of $(X)_{\text{sil}}$ from the measured major ion abundances is model dependent and relies on the use of suitable proxy (Na^+ , Ca^{2+} and Mg^{2+} , K^+) and assumptions regarding the release of various elements from rocks to water (Singh et al. 1998; Galy and France-Lanord 1999; Dalai et al. 2002). Sodium is hosted almost exclusively in silicate minerals, which makes it a useful proxy for silicate weathering. For this study, we have chosen Na^+ as proxy based on their dominance in groundwater. A common proxy is Na_{sil} , which is calculated as:

$$\text{Na}_{\text{sil}}^+ = \text{Na}_{\text{GW}}^+ - (\text{Na}_{\text{rain}}^+ + \text{Na}_{\text{as}}^+) \tag{4}$$

where subscripts “sil, GW, rain and as” refer to silicates, groundwater, rainwater and anthropogenic inputs. The Na_{rain} depicts rainwater concentration of Na^+ appropriately corrected for evapotranspiration. Often $(\text{Na}_{\text{rain}} + \text{Na}_{\text{as}})$ is approximated as equal to

measured Cl^- in groundwater, Cl_{GW}^- . This makes Na_{sil}^+ equal to:

$$[\text{Na}^+]_{\text{sil}} \approx (\text{Na}_{\text{GW}}^+ - \text{Cl}_{\text{GW}}^-). \quad (5)$$

In case of K, its dominant source is silicate weathering with minor supply from rains; therefore, K_{sil}^+ can be calculated by subtracting the rainwater K contribution from measured values in groundwater. For Ca^{2+} and Mg^{2+} , their silicate components (Ca_{sil} , Mg_{sil}) are difficult to estimate as they have several sources; hence, mineralogical compositions of litho-units of the study area are considered (Singh et al. 1998). In groundwater, Ca_{sil} and Mg_{sil} are calculated by assuming that they are released into the groundwater from silicates in a fixed proportion relative to Na (Gaillardet et al. 1999). The $(\text{Ca}^{2+})_{\text{sil}}$ and $(\text{Mg}^{2+})_{\text{sil}}$ can be calculated by the following formulas:

$$[\text{Ca}^{2+}]_{\text{sil}} = [\text{Na}^+]_{\text{sil}} \times [\text{Ca}^{2+}/\text{Na}^+]_{\text{rock}} \quad (6)$$

$$[\text{Mg}^{2+}]_{\text{sil}} = [\text{Na}^+]_{\text{sil}} \times [\text{Mg}^{2+}/\text{Na}^+]_{\text{rock}} \quad (7)$$

where Na_{sil} is the weighted mean sodium concentration of groundwater corrected from atmospheric inputs, subscripts “sil” refers to silicate origin and “rock” refers to bedrock composition. The average rock composition from the litho-units (CHK and HBG) was considered for the calculation. The $[\text{Ca}^{2+}/\text{Na}^+]_{\text{rock}}$ and $[\text{Mg}^{2+}/\text{Na}^+]_{\text{rock}}$ are the ratios from which the Ca^{2+} and Mg^{2+} released relative to Na from parent rock to groundwater can be determined. The calculations are attempted, assuming that the said elements are released into groundwater in the same ratio as their abundances in bedrock. The calculated molar ratio of $\text{Ca}^{2+}/\text{Na}^+$ in CHK is 0.47 and in HBG is 0.35 and the ratio of $\text{Mg}^{2+}/\text{Na}^+$ in CHK and HBG is as 0.24 and 0.41, respectively. The calculated SWR for CHK is $3.07 \text{ tons km}^{-2} \text{ year}^{-1}$ and for HBG is $5.12 \text{ tons km}^{-2} \text{ year}^{-1}$. Weathering is more rapid in HBG in comparison with CHK, which might be due to consequence of mineral weathering from the litho-units of the study area. The weathering rate variations in HBG and CHK trends are controlled not only by mineralogy but by the differences in texture of the rocks also (Drever 1988).

The carbonate weathering rate (CWR) $\text{tons km}^{-2} \text{ year}^{-1}$ is calculated for individual litho-units based on the equation proposed by Roy et al. (1999):

$$\text{CWR} = (\text{Ca}_{\text{carb}}^{2+} + \text{Mg}_{\text{carb}}^{2+} + 0.5(\text{HCO}_3^-)) \times Q/A/\text{density of Carbonate} \quad (8)$$

where Q is the discharge in $\text{m}^3 \text{ Year}^{-1}$, A is the total surface area in km^2 and Ca_{carb} and Mg_{carb} represent the cations supplied by carbonates (mg L^{-1}) (Krishnaswami et al. 2005). The average density of carbonate considered is 2400 Kg m^{-3} (Galy and France-Lanord 1999). The supply of Ca and Mg ions from carbonates can be calculated by the equations given as follows:

$$\text{Ca}_{\text{carb}}^{2+} = \text{Ca}_{\text{GW}}^{2+} - \text{Ca}_{\text{sil}}^{2+} \quad (9)$$

$$\text{Mg}_{\text{carb}}^{2+} = \text{Mg}_{\text{GW}}^{2+} - \text{Mg}_{\text{sil}}^{2+}. \quad (10)$$

The subscript “carb” refers to carbonate contribution and the Ca_{GW} and Mg_{GW} have already been corrected for atmospheric contributions. The calculated carbonate weathering in CHK and HBG is $0.079 \text{ tons km}^{-2} \text{ year}^{-1}$ and $0.74 \text{ tons km}^{-2} \text{ year}^{-1}$, respectively. Silicate weathering rate calculated for CHK and HBG was $3.07 \text{ tons km}^{-2} \text{ year}^{-1}$ and $5.12 \text{ tons km}^{-2} \text{ year}^{-1}$, respectively. The calculated carbonate weathering rate in CHK and HBG was $0.079 \text{ tons km}^{-2} \text{ year}^{-1}$ and $0.74 \text{ tons km}^{-2} \text{ year}^{-1}$, respectively. Comparing HBG and CHK, the HBG is the prominent rock type enriched with silicate minerals which are comparatively higher than the carbonate minerals in composition. These gneisses exhibit numerous features such as lineation, folds and weak planes like fractures that ease the percolation of groundwater (Vyshnavi and Islam 2015). Hence, HBG is more prone to silicate weathering due to its distinct mineralogy, especially feldspar and mica which are more susceptible to weathering. Dissolved chemical constituents in Shanmuganadhi are dominantly originated from the chemical weathering of silicate rocks and also by minor contribution from carbonate weathering. Therefore, the study domain signifies the dominance of silicate weathering which is accounted for by two favouring conditions. The primal is the silicate rock abundance, and as per Datta and Tyagi (1996), carbonate weathering processes are also responsible for Ca^{2+} , Mg^{2+} , HCO_3^- and SO_4^{2-} in the groundwater along with silicate weathering.

The predominance of silicate or carbonate weathering can be inferred from Ca–Mg–(Na + K) ternary diagram. The ternary diagram contains details about

phase behaviour of mixture of three components (Na + K, Ca and Mg) in a triangular diagram (Krishnan et al. 2012). Silicate weathering results in sample clustering close to (Na + K) apex and carbonate weathering results in samples close to Ca or (Mg) apex (Pattanaik et al. 2013). If the samples points plot in the centre of the ternary diagram, it is inferred that both silicate and carbonate weathering had contributed to the solutes in groundwater (Blum et al. 1998). The plot for the study area (Fig. 6) infers groundwater dominated by silicate weathering brought about mainly by weathering of alkali feldspar which releases Na⁺ and K⁺ ions, and therefore, groundwater samples plot close to the (Na + K) apex in the study area.

Carbon dioxide consumption by chemical weathering

Atmospheric CO₂ has steadily increased since 1850 and is currently increasing at a rate of 0.5% year (Lal et al. 2001), stimulating investigations into the numerous reservoirs and fluxes within the global CO₂ cycle. Chemical weathering is the main natural mechanism limiting the atmospheric carbon dioxide levels on geologic timescales (> 1 Ma) (Beaulieu

et al. 2012). The atmospheric carbon consumed by weathering is returned to the atmosphere through several processes: (1) CO₂ consumed by weathering of carbonates in the continents is completely reverted to the atmosphere through carbonate precipitation in the ocean; (2) half of the CO₂ consumed during weathering of Ca²⁺ and Mg²⁺ silicates is precipitated as CaCO₃ and half is released back into the atmosphere as CO₂; (3) Na⁺ and K⁺ ions may undergo reverse weathering to form authigenic clays and CO₂ (Walker et al. 1981a, b; Berner et al. 1983). The effect of carbonate weathering on atmospheric CO₂ is slightly different than that of silicate weathering. The weathering reactions of silicate mineral hydrolysis and carbonate dissolution consume atmospheric carbon dioxide and increase alkalinity of the solution (Mortatti and Probst 2003), as portrayed by reactions noted in the following:

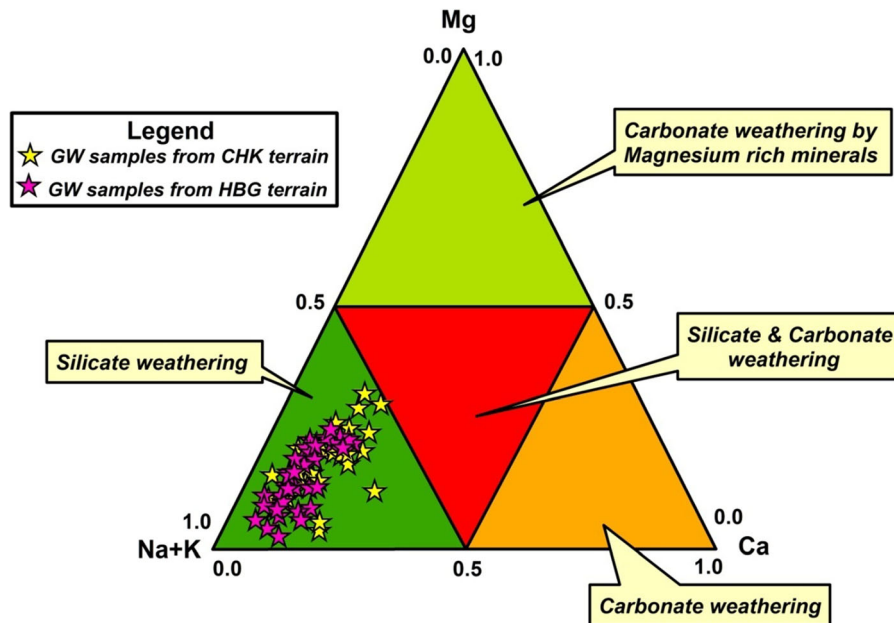
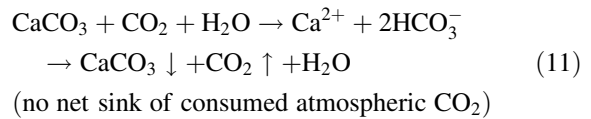
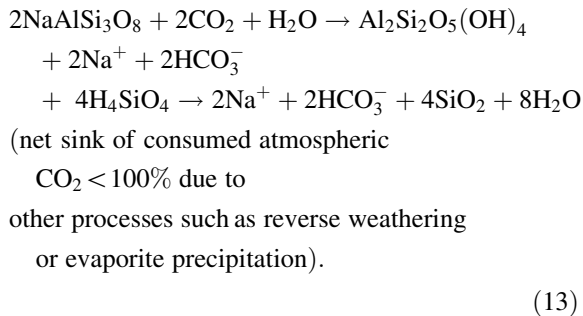
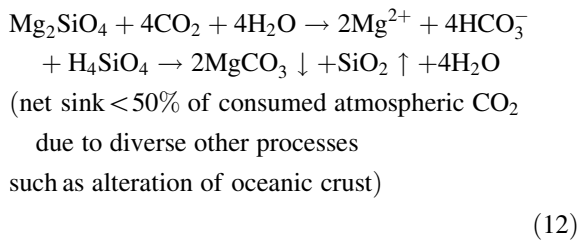


Fig. 6 Calcium–magnesium–(sodium + potassium) ternary diagram



The above reactions are simplified that describe reactions for the dissolution of simple carbonate and silicate minerals, illustrating the “consumption” of CO₂ during weathering aided by carbonic acid (Hartmann and Kempe 2008; Truesdell and Jones 1973). Chemical weathering in geological units is significant for accounting net loss of atmospheric CO₂ depending on diverse geological timescales. With respect to million-year timescale, in ocean marine life incorporates the Ca²⁺ and HCO₃⁻ ions into CaCO₃ and again it liberates CO₂, which eventually escapes into the atmosphere (Gaillardet et al. 1999). Hence, during the carbonate weathering there is no net loss of atmospheric CO₂. The carbon dioxide consumption rate can be calculated using major element concentrations, mean annual discharge and drainage basin area. For the estimation of CO₂ flux consumed by chemical weathering parameters such as hydrological, geographical and geological features incorporating mean elevation, basin area of the drainage and surface area of litho-units confined to the study area were considered in GIS environment. The CO₂ consumption rate due to silicate weathering is computed as the flux of total dissolved cations from silicate weathering. The CO₂ consumption rate has been attempted by considering the equations suggested by Gurusurthy et al. 2012) as noted below:

$$\begin{aligned} \text{Carbonate Consumption Rate (CCR)} \\ = Q/A \times (\text{Na}_{\text{Sil}}^+ + \text{K}_{\text{Sil}}^+ + \text{Ca}_{\text{Sil}}^{2+} + \text{Mg}_{\text{Sil}}^{2+}) \end{aligned} \quad (14)$$

where Q is the discharge, A is the drainage area and subscript “Sil” refers to cations derived from the silicate weathering. Uptake of CO₂ by carbonate weathering is not included because it is not a net sink of atmospheric CO₂ on timescales longer than 1 my (Lingling et al. 2005). The CCR in CHK during silicate weathering is calculated as 1.4×10^3 mol km⁻² year⁻¹ and in HBG as 5.8×10^3 mol km⁻² year⁻¹. The flux of CO₂ consumed by rock weathering is greatly variable according to rock types. Higher CCR is noted in HBG than in CHK, which might be due to the influence of difference in degree of silicate rock weathering confined to the study area. Disproportionately higher CO₂ drawdown via silicate weathering in HBG could result from enhanced silicate weathering driven by orographic precipitation, relief and environmental factors (Raymo and Ruddiman 1992). The CO₂ consumption caused by silicate weathering regulates the atmospheric CO₂ level and constitutes a significant part of the global carbon budget (Xiaoxi Lyu et al. 2009; Kenoyer and Bowser 1992).

Spatial pattern of SWR and CCR in groundwater

To understand the spatial pattern of SWR in the study area, the sum of weathering rate is plotted in ARG GIS platform (Fig. 7a). The influence of weathering in groundwater is related to degree of rock mass weathering. According to British Standards—BS 5930 (1981), rate of weathering is categorized into three classes as slightly weathered, moderately weathered and highly weathered. Higher weathering rate is observed along the northern parts of the study area, moderate weathering is confined to central and northern parts of the study region where exposure of HBG is noted, and slight weathering is noted along the southern, north-western, north-eastern regions and central parts of the study area in locations of CHK exposures. The rate of weathering seems to be influenced by the presence of fractures along with favourable morphological feature exposures confined to the study area. Rate of chemical weathering seems to be regulated by mineral surface area, temperature, leaching intensity (availability of water) and mineral composition. The presence of CHK in the study area is confined to higher elevations when compared with

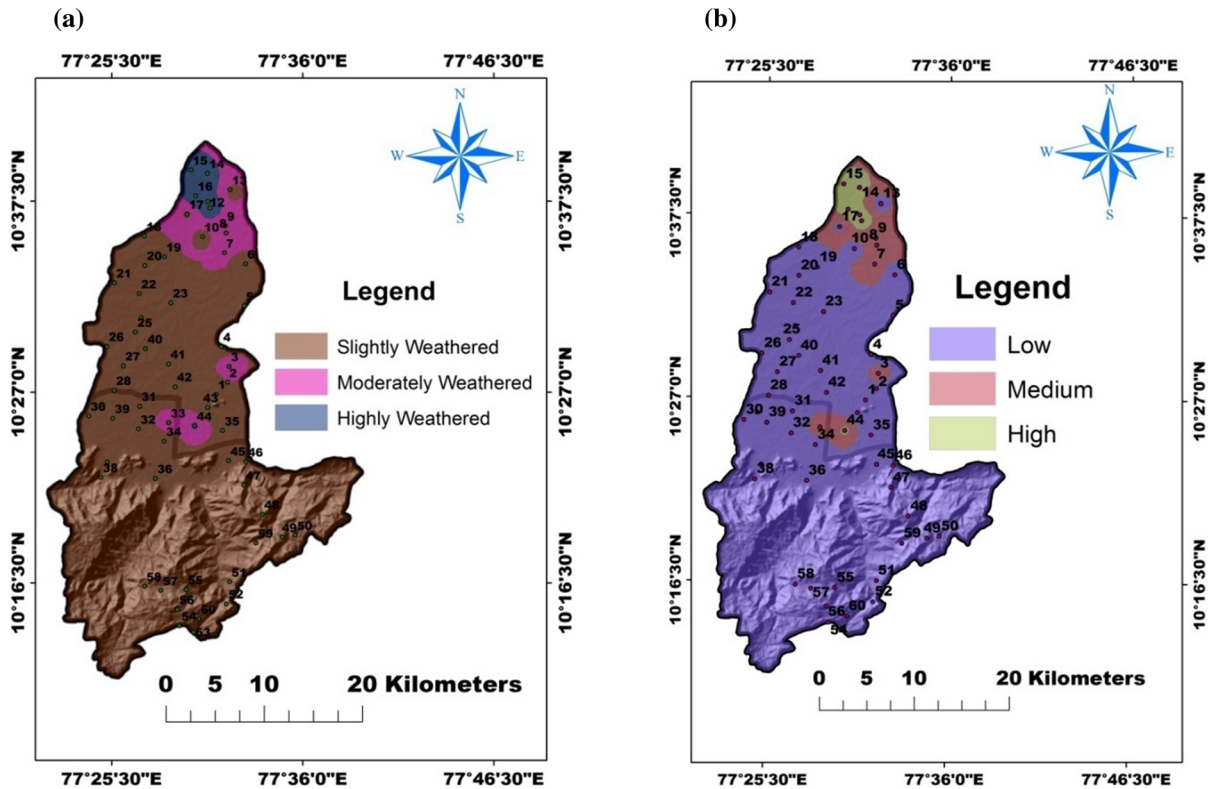


Fig. 7 a and b Spatial distribution map for SWR and CCR

HBG. Hence, CHK shows lesser influence of chemical weathering in comparison with HBG, which might be due to their massive nature which restricts the degree of weathering. Irrespective of varying lithology but with less significant mineralogy, the geochemical characteristics of chemical weathering varied ominously where CHK is found to be chemical less reactive in comparison with HBG. Higher weathering rates noted in HBG result in additional geochemical reactivity of minerals. From the CCR spatial plot (Fig. 7b), it is noted that higher rate of carbon dioxide consumption is distributed along the northern parts of the study area followed by medium consumption noted in central and northern parts and lower consumption rates confined to southern, north-western, north-eastern and central parts of the study area. The above result signifies higher CO₂ consumption in HBG when compared with CHK. The subtropical climatic condition along with dominant silicate lithology leads to higher carbon dioxide consumption rate confined to Shanmuganadhi sub-basin irrespective of litho-units.

Comparison of present SWR, CWR and CO₂ consumption with global studies

Attempt has also been made to compare the present SWR, CWR and CO₂ consumption rates with global studies (Table 2). SWR, CWR and carbon dioxide consumption rate calculated for charnockite and hornblende–biotite gneiss were 3.07 tons km⁻² year⁻¹ and 5.12 tons km⁻² year⁻¹, 0.079 tons km⁻² year⁻¹ and 0.74 tons km⁻² year⁻¹, and the calculated CO₂ consumption rate via silicate weathering was 1.4 × 10³ mol km⁻² year⁻¹ and 5.8 × 10³ mol km⁻² year⁻¹ for CHK and HBG, respectively. The SWR calculated for the Himalayan River system such as the Ganga River ranges between 10.2 and 15.2 tons km⁻² a⁻¹ (Krishnaswami et al. 2005; Dalai et al. 2002). The SWR and carbon dioxide consumption rate via silicate weathering in the Brahmaputra were 10.32 tons km⁻² a⁻¹ and 4.9 × 10⁵ mol km⁻² year⁻¹, respectively (Gaillardet et al. 1999; Macpherson et al. 2008). The SWR and carbon dioxide consumption rate via silicate weathering in Indus were 3.8 tons km⁻² a⁻¹ and

Table 2 Comparison of rates in Shanmuganadhi sub-basin with global studies

Study site	Water type	Methodology	Rates			References
			SWR	CWR	CCR via SWR	
Musuri, India	RW	Mass balance	9.44	1.46	3.83×10^5	Pattanaik et al. (Pattanaik et al. 2013)
Ganga, India	RW	Mass balance	10.2–15.2	–	–	Krishnaswami et al. (1999)
Brahmaputra, India	RW	Mass balance	10.32	–	4.9×10^5	Gaillardet et al. (1999)
Indus, India	RW	Mass balance	9.44	–	0.6×10^5	Gaillardet et al. (1999)
Seine River, Paris	RW	Mass balance	2	48	$15\text{--}24 \times 10^3$	Roy et al. (1999)
Liwu, Taiwan	GW	Mass balance	6.9	–	–	Calmels et al. (2011)
Shanmuganadhi, India	GW	Mass balance	CHK-3.07	0.079	1.4×10^3	This study
			HBG-5.12	0.74	5.8×10^3	

SWR and CWR in $\text{tons km}^{-2} \text{ year}^{-1}$, CCR in $\text{mol/km}^2/\text{yr}$

RW river water, GW ground water

$0.6 \times 10^5 \text{ mol km}^{-2} \text{ year}^{-1}$, respectively (Krishnaswami et al. 1999) (Gaillardet et al. 1999). The annual SWR, CWR and carbon dioxide consumption rate via silicate weathering in the Musuri, India, were $9.44 \text{ tons km}^{-2} \text{ a}^{-1}$, $1.46 \text{ tons km}^{-2} \text{ a}^{-1}$ and $3.83 \times 10^5 \text{ mol km}^{-2} \text{ year}^{-1}$, respectively (Gaillardet et al. 1999). The SWR, CWR and carbon dioxide consumption rate via silicate weathering in Seine River, France, were $2 \text{ tons km}^{-2} \text{ year}^{-1}$, $48 \text{ tons km}^{-2} \text{ year}^{-1}$ and $15\text{--}24 \times 10^3 \text{ mol km}^{-2} \text{ year}^{-1}$, respectively (Roy et al. 1999). The variations in rate might be attributed to variation in surface area, climate, vegetation, exposure of the parent rock lithology, precipitation and intense runoff.

Conclusion

The study indicates dominance of chemical weathering over other processes responsible for the geochemistry of groundwater. Irrespective of lithology, pH in groundwater represents alkaline nature. The dominance of major ions in groundwater was in the order of $\text{Na}^+ > \text{Ca}^{2+} > \text{Mg}^{2+} > \text{K}^+ > \text{NH}_4^+$ and $\text{Cl}^- > \text{HCO}_3^- > \text{SO}_4^{2-} > \text{NO}_3^- > \text{PO}_4^{2-} > \text{F}^-$. Irrespective of litho-units, major groundwater facies isolated were mixed $\text{Ca}^{2+}\text{Mg}^{2+}\text{Cl}^-$ and $\text{Na}^+\text{--Cl}^-$ types with minor representations of $\text{Ca}^{2+}\text{--HCO}_3^-$ and $\text{Ca}^{2+}\text{Na}^+$ types. The hydrogeochemical facies indicate rock–water interaction, leading to weathering and dissolution of rock types such as HBG and CHK, leading to

the release of ions such as Ca^{2+} , Mg^{2+} , Na^+ and K^+ in groundwater, resulting from weathering of pyroxenes, amphiboles, feldspars and biotite. The ionic ratio plots suggest silicate weathering and carbonate dissolution processes to be activated in the study area. An increase in SI of minerals along the groundwater flow path signifies the influence of lithological sources for the alteration in the water chemistry. Saturation index of minerals along the groundwater flow path gave significant results in view of geochemical evolution of groundwater geochemistry. In HBG, SI of silicate is high when compared with CHK, indicating groundwater flow from recharge to discharge area alters the saturation index of mineral phases. The estimated silicate weathering rate in CHK and HBG was 3.07 and 5.12 $\text{tons km}^{-2} \text{ year}^{-1}$, respectively, and the calculated carbonate weathering rate in charnockite and hornblende–biotite gneiss was 0.079 $\text{tons km}^{-2} \text{ year}^{-1}$ and 0.74 $\text{tons km}^{-2} \text{ year}^{-1}$, respectively. The carbon dioxide consumption rate calculated for CHK and HBG was $1.4 \times 10^3 \text{ mol km}^{-2} \text{ year}^{-1}$ and $5.8 \times 10^3 \text{ mol km}^{-2} \text{ year}^{-1}$, respectively. The humid subtropical condition along with dominant silicate lithology signifies higher carbon dioxide consumption rate during weathering process confined to the study area. The present study reveals natural weathering process is dominate in the study area. The present investigation demonstrates the major hydrogeochemical and minor anthropogenic processes responsible for aquifer chemistry in the region, which in turn may

help in the groundwater quality management and decision-making in the study area.

Acknowledgements The corresponding author acknowledges support from Pondicherry University Research fellowship. The authors are grateful to two anonymous reviewers for their insightful comments on the manuscript, as the comments directed us to improve the work in the present form.

References

APHA. (2005). *Standard methods for the examination of water and wastewater* (21st ed.). Washington, DC: American Public Health Association/American Water Works Association/Water Environment Federation.

Aravinthasamy, P., Karunanidhi, D., Subramani, T., Srinivasamoorthy, K., & Anand, B. (2019). Geochemical evaluation of fluoride contamination in groundwater from Shanmuganadhi River basin, South India: implication on human health. *Environmental Geochemistry and Health*. <https://doi.org/10.1007/s10653-019-00452-X>.

Arditto, P. (1983). Mineral-groundwater interactions and the formation of authigenic kaolinite within the southeastern intake beds of the Great Australian (Artesian) Basin, New South Wales, Australia. *Sedimentary Geology*, 35(4), 249–261. [https://doi.org/10.1016/0037-0738\(83\)90061-1](https://doi.org/10.1016/0037-0738(83)90061-1).

Ball, J. W., Nordstrom, D. K., & Zachmann, D. W. (1987). WATEQ4F—A personal computer FORTRAN translation of the geochemical model WATEQ2 with revised data base: U.S. Geological Survey Open-File Report, 87-50, 108. <https://www.researchgate.net/publication/236246808>.

Basavarajappa, H. T., & Manjunatha, M. C. (2015). Groundwater quality analysis in Precambrian rocks of Chitradurga district, Karnataka, India using Geo informatics technique. *Aquatic Procedia*, 4, 1354–1365. <https://doi.org/10.1016/j.aqpro.2015.02.176>.

Beaulieu, E., Godderis, Y., Donnadieu, Y., Labat, D., & Roelandt, C. (2012). High sensitivity of the continental-weathering carbon dioxide sinks to future climate change. *Nature Climate Change*, 2, 346–349. <https://doi.org/10.1038/nClimate1419>.

Berg, G. (1932). *Das Vorkommen der chemischen Elementen auf der Erde* (p. 204). Leipzig: Johan Ambrosius Barth.

Berner, R. A. (1991). A model for atmospheric CO₂ over Phanerozoic time. *American Journal of Science*, 291, 339–376. <https://doi.org/10.2475/ajs.291.4.339>.

Berner, R. A., Lassaga, A. C., & Garrels, R. M. (1983). The carbonate–silicate geochemical cycle and its effect on atmospheric carbon dioxide over the past 100 million years. *American Journal Science*, 284, 1183–1192. <https://doi.org/10.2475/ajs.283.7.641>.

BIS 5930. (1981). *Code of practice for site investigations, British standard* (Vol. 152). London: British Standards Institution.

Blum, J. D., Gazis, C. A., Jacobson, A. D., & Chamberlain, C. P. (1998). Carbonate versus silicate weathering in Raikhot

watershed within the High Himalayan crystalline series. *Geology*, 26, 411–414.

Böhlke, J. K., Smith, R. L., & Miller, D. N. (2006). Ammonium transport and reaction in contaminated groundwater: application of isotope tracers and isotope fractionation studies. *Water Resources Research*. <https://doi.org/10.1029/2005WR004349>.

Brookins, D. G. (1988). *Eh-pH diagrams for geochemistry* (pp. 116–117). Berlin: Springer. <https://doi.org/10.1007/978-3-642-73093-147>.

Calmels, D., Galy, A., Hovius, N., Bickle, M., West, A. J., Chen, M. C., et al. (2011). Contribution of deep groundwater to the weathering budget in a rapidly eroding mountain belt, Taiwan. *Earth and Planetary Science Letters*, 303, 48–58. <https://doi.org/10.1016/j.epsl.2010.12.032>.

CGWB. (2008). Central Groundwater Board, Annual Report. South Eastern Coastal Region, Government of India.

Clayton, J. L. (1988). Some observations on the stoichiometry of feldspar hydrolysis in granitic soil. *Journal Environmental Quality*, 17, 153–157.

Corbett, R. G. (1979). Geology and water characteristics. In W. M. Edmunds & P. L. Smedley (Eds.), *Geochemistry of water in cardiovascular disease* (pp. 14–38), Panel on the geochemistry of water in relation to cardiovascular diseases Washington, D.C.: National Academy of Sciences.

Dalai, T. K., Krishnaswami, S., & Sarin, M. M. (2002). Major ion chemistry in the headwaters of the Yamuna river system: Chemical weathering, its temperature dependence and CO₂ consumption rates. *Geochimica et Cosmochimica Acta*, 66(19), 3397–3416. [https://doi.org/10.1016/S0016-7037\(02\)00937-7](https://doi.org/10.1016/S0016-7037(02)00937-7).

Das, B. K., & Kaur, P. (2001). Major ion chemistry of Renuka lake and weathering processes, Sirmaur district, Himachal Pradesh, India. *Journal of Environmental Geology*, 40, 908–917. <https://doi.org/10.1007/s12665-019-8315-z>.

Das, A., Krishnaswami, S., Sarin, M. M., & Pande, K. (2005). Chemical weathering in the Krishna basin and the western ghats of the Deccan Traps: Rates of weathering and their control. *Geochimica et Cosmochimica Acta*, 69, 2067–2084. <https://doi.org/10.1016/j.gca.2004.10.014>.

Datta, P. S., & Tyagi, S. K. (1996). Major ion chemistry of groundwater in Delhi area: Chemical weathering processes and groundwater regime. *Journal of the Geological Society of India*, 47(2), 179–188.

Donnini, M., Frondini, F., Probst, J.-L., Probst, A., Cardellini, C., Marchesini, I., et al. (2016). Chemical weathering and consumption of atmospheric carbon dioxide in the Alpine region. *Global and Planetary Change*, 136, 65–81. <https://doi.org/10.1016/j.gloplacha.2015.10.017>.

Drever, J. I. (1988). *The geochemistry of natural waters* (2nd ed., p. 437). Englewood Cliffs: Prentice-Hall.

Duraisamy, S., Govindhaswamy, V., Duraisamy, K., Krishnaraj, S., Balasubramanian, A., & Thirumalaisamy, S. (2018). Hydrogeochemical characterization and evaluation of groundwater quality in Kangayam taluk, Tirupur district, Tamil Nadu, India, using GIS techniques. *Environmental Geochemistry and Health*, 41(2), 851–873. <https://doi.org/10.1007/s10653-018-0183-z>.

Elango, L., Kannan, R., & Senthil Kumar, M. (2003). Major ion chemistry and identification of hydrogeochemical processes of groundwater in a part of Kancheepuram district,

- Tamil Nadu, India. *Journal of Environmental Geoscience*, 10, 157–166. <https://doi.org/10.1306/eg100403011>.
- Fisher, S. R., & Mullican, W. F. (1997). Hydrochemical evolution of sodium-sulfate and sodium-chloride groundwater beneath the Northern Chihuahuan Desert, Trans-Pecos, Texas, USA. *Hydrogeology Journal*, 5, 4–16. <https://doi.org/10.1007/s100400050102>.
- Fuller, W. H. (1951). Soil organic matter. In R. L. Cook & B. G. Ellis (Eds.), *Soil management: A world view of conservation and production* (pp. 152–170). New York: Wiley.
- Gaillardet, J., Dupre, B., & Allegre, C. J. (1999). Global silicate weathering and CO₂ consumption rates deduced from the chemistry of large rivers. *Chemical Geology*, 159, 3–30. [https://doi.org/10.1016/S0009-2541\(99\)00031-5](https://doi.org/10.1016/S0009-2541(99)00031-5).
- Galy, A., & France-Lanord, C. (1999). Weathering processes in the Ganges–Brahmaputra basin and the riverine alkalinity budget. *Chemical Geology*, 159, 31–60.
- Garrels, R. M., & Mackenzie, F. T. (1967). Origin of the chemical compositions of some springs and lakes. In W. Stumm (Ed.), *Equilibrium concepts in natural water systems*. Advances in Chemistry Series (Vol 67, pp. 222–242).
- Ghandour, E. I. M., Khalil, J. B., & Atta, S. A. (1985). Distribution of carbonates, bicarbonates and pH values in groundwater of the Nile delta region, Egypt. *Groundwater*, 23, 35–41. <https://doi.org/10.1111/j.1745-6584.1985.tb02777.x>.
- Gislason, S. R., Arnorsson, S., & Armannsson, H. (1996). Chemical weathering of basalt in Southwest Iceland: Effects of runoff, age of rocks and vegetative/glacial cover. *American Journal of Science*, 296, 837–907. <https://doi.org/10.2475/ajs.296.8.837>.
- Glover, E. T., Akiti, T. T., & Osaе, S. (2012). Major ion chemistry and identification of geochemical processes of groundwater in the Accra Plains. *Geoscience*, 50, 10279–10288.
- Guilbert, P. A., & Dejoy, A. L. (1979). Phosphorus in the environment: Its chemistry and biochemistry. The Use of Phosphate Detergents and Possible Replacements for Phosphate, CIBA Foundation Symposium 57: Amsterdam. <https://doi.org/10.1002/9780470720387.ch14>.
- Guo, S., Wang, J., Xiong, L., Ying, A., & Li, D. (2002). A macro-scale and semi-distributed monthly water balance model to predict climate change impacts in China. *Journal of Hydrology*, 2002(268), 1–15. [https://doi.org/10.1016/S0022-1694\(02\)00075-6](https://doi.org/10.1016/S0022-1694(02)00075-6).
- Gurumurthy, G. P., Balakrishna, K., Riotte, J., Braun, J.-J., Audry, S., Shankar, H. N. U., et al. (2012). Controls on intense silicate weathering in a tropical river, southwestern India. *Chemical Geology*, 300–301, 61–69. <https://doi.org/10.1016/j.chemgeo.2012.01.016>.
- Hargreaves, G. H., & Allen, R. G. (2003). History and evaluation of Hargreaves evapotranspiration equation. *Journal of Irrigation and Drainage Engineering*, 129, 53–63. [https://doi.org/10.1061/\(ASCE\)b0733-9437\(2003\)129:1\(53\)](https://doi.org/10.1061/(ASCE)b0733-9437(2003)129:1(53)).
- Hartmann, J., & Kempe, S. (2008). What is the maximum potential for CO₂ sequestration by stimulated weathering on the global scale. *Naturwissenschaften*, 95, 1159–1164. <https://doi.org/10.1007/s00114-008-0434-4>.
- Hem, J. D. (1985). *Study and interpretation of the chemical characteristics of natural water* (3rd ed., Vol. 2254). Reston: US Geological Survey, Water Supply.
- Hounslow, A. W. (1995). *Water quality data: Analysis and interpretation* (Vol. 416). Boca Raton: CRC Press LLC, Lewis Publishers. <https://doi.org/10.1201/9780203734117>.
- Huang, S.-b., Han, Z.-t., Zhao, L., & Kong, X.-K. (2015). Risk assessment and prediction of heavy metal pollution in groundwater and river sediment: A case study of a typical agricultural irrigation area in Northeast China. *International Journal of Analytical Chemistry*. <https://doi.org/10.1155/2015/921539>.
- Karunanidhi, D., Aravinthasamy, P., Subramani, T., Wu, J., & Srinivasamoorthy, K. (2019). Potential health risk assessment for fluoride and nitrate contamination in hard rock aquifers of Shanmuganadhi River basin, South India. *Human and Ecological Risk Assessment*, 25(1–2), 250–270. <https://doi.org/10.1080/10807039.2019.1568859>.
- Karunanidhi, D., Vennila, G., Suresh, M., & Subramanian, S. K. (2013). Evaluation of the groundwater quality feasibility zones for irrigational purposes through GIS in Omalur Taluk, Salem District, South India. *Environmental Science and Pollution Research*, 20(10), 7320–7333. <https://doi.org/10.1007/s11356-013-1746-2>.
- Katz, B. G., Bricker, O. P., & Kennedy, M. M. (1985). Geochemical mass-balance relationships for selected ions in precipitation and stream water, Catocin Mountains, Maryland. *American Journal Science*, 285, 931–962. <https://doi.org/10.2475/ajs.285.10.931>.
- Kenoyer, G. J., & Bowser, C. J. (1992). Groundwater chemical evolution in a sandy silicate aquifer in northern Wisconsin: 1. Patterns and rates of change. *Water Resources Research*, 28(2), 579–589. <https://doi.org/10.1029/91WR02302>.
- Krishnan, A. S., Smith, S. D., & Spontak, R. J. (2012). Ternary phase behavior of a triblock copolymer in the presence of an endblock-selective homopolymer and midblock-selective oil. *American Chemical Society*, 45(15), 6056–6067. <https://doi.org/10.1021/ma300417u>.
- Krishnaswami, S., & Singh, S. K. (2005). Chemical weathering in the river basins of the Himalaya, India. *Current Science*, 89(5), 841–884.
- Krishnaswami, S., Singh S. K., & Dalai T. K. (1999). Silicate weathering in the Himalaya: Role in contributing to major ions and radiogenic Sr to the Bay of Bengal. In B. L. K. Somayajulu (Ed.), *Ocean science, trends and future directions* (pp. 23–51). Indian National Science Academy and Akademia International.
- Lakshmanan, E., Kannan, R., & Senthil Kumar, M. (2003). Major ion chemistry and identification of hydrogeochemical processes of ground water in a part of Kancheepuram district, Tamil Nadu, India. *Environmental Geosciences*, 10, 157–166. <https://doi.org/10.1306/eg100403011>.
- Lal, M., Nozawa, T., Emori, S., Harasawa, H., Takahashi, K., Kimoto, M., et al. (2001). Future climate change: Implications for Indian summer monsoon and its variability'. *Current Science*, 81, 1196–1207.
- Lerman, A., Lingling, W., & Fred, M. T. (2007). CO₂ and H₂SO₄ consumption in weathering and material transport to the ocean, and their role in the global carbon balance.

- Marine Chemistry*, 106, 326–350. <https://doi.org/10.1016/j.marchem.2006.04.004>.
- Lingling, W., Youngdook, H., Janhua, Q., Gu, D., & Der Lee, S. (2005). Chemical weathering in the Upper Huang He (Yellow River) draining the eastern Qinghai-Tibet Plateau. *Geochimica et Cosmochimica Acta*, 69(22), 5279–5294. <https://doi.org/10.1016/j.gca.2005.07.001>.
- Liu, Z. J., Liu, Y. S., & Li, Y. R. (2018). Anthropogenic contributions dominate trends of vegetation cover change over the farming-pastoral ecotone of northern China. *Ecological Indicators*, 95, 370–378. <https://doi.org/10.1016/j.ecolind.2018.07.063>.
- Lyu, X., Tao, Z., Gao, Q., Peng, H., & Zhou, M. (2009). Chemical weathering and riverine carbonate system driven by human activities in a subtropical Karst Basin, South China. *Water*, 10, 1524. <https://doi.org/10.3390/w10111524>.
- Macpherson, G. L., Roberts, J. A., Blair, J. M., Townsend, M. A., Fowle, D. A., & Beisner, K. R. (2008). Increasing shallow groundwater CO₂ and limestone weathering, Konza Prairie, USA. *Geochimica et Cosmochimica Acta*, 72, 5581–5599. <https://doi.org/10.1016/j.gca.2008.09.004>.
- Maher, K., & Chamberlain, C. P. (2014). Hydrologic regulation of chemical weathering and the geologic carbon cycle. *Sciences*, 343(6178), 1502–1504. <https://doi.org/10.1126/science.1250770>.
- Mattson, M. D. (2014). Alkalinity of fresh water. *Reference Module in Earth Systems and Environmental Sciences*. <https://doi.org/10.1016/B978-0-12-409548-9.09397-0>.
- Nakagawa, K., Amano, H., Asakura, H., & Berndtsson, R. (2016). Spatial trends of nitrate pollution and groundwater chemistry in Shimabara, Nagasaki, Japan. *Environmental Earth Sciences*, 75(3), 1–17. <https://doi.org/10.1007/s12665-015-4971-9>.
- Olobaniyi, S. B., Ogala, J. E., & Nfor, N. B. (2007). Hydro-geochemical and bacteriology investigation of groundwater in Agbor area, southern Nigeria. *Journal of Mining and Geology*, 43(1), 79–89. <https://doi.org/10.4314/jmg.v43i1.18867>.
- Pacheco, F., & Van der Weijden, C. H. (1996). Contributions of water–rock interactions to the composition of groundwaters in areas with a sizeable anthropogenic input: a case study of the water of the Fundao area, central Portugal. *Water Resources Research*, 32(12), 3553–3570. <https://doi.org/10.1029/96WR01683>.
- Pande, K., Sarin, M. M., Trivedi, J. R., Krishnaswami, S., & Sharma, K. K. (1994). The Indus river system (India-Pakistan): Major-ion chemistry, uranium and strontium isotopes. *Chemical Geology*, 116, 245–259.
- Parkhurst, D. L., Plummer, L. N., & Thorstenson, D. C. (1982). BALANCE—A computer program for calculating mass transfer for geochemical reactions in ground water: U.S. Geological Survey Water-Resources Investigations 82-14, 29.
- Parkhurst, D. L., Thorstenson, D.C., & Plummer, L.N. (1980). PHREEQE—A computer program for geochemical calculations: U.S. Geological Survey Water-Resources Investigations, 80-96, 193.
- Pattanaik, J., Balakrishnan, S., Bhutani, R., & Singh, P. (2013). Estimation of weathering rates and CO₂ drawdown based on solute load: Significance of granulites and gneisses dominated weathering in the Kaveri River basin, Southern India. *Geochimica et Cosmochimica Acta*, 121, 611–636. <https://doi.org/10.1016/j.gca.2013.08.002>.
- Piper, A. M. (1944). A graphical procedure in the geochemical interpretation of water analysis. *Transactions, American Geophysical Union*, 25, 914–928.
- Plummer, L. N., Bexfield, L. M., Anderholm, S. K., Sanford, W. E., & Busenberg, E. (2004). Hydrochemical tracers in the Middle Rio Grande Basin, USA: 1. Conceptualization of groundwater flow. *Hydrogeol Journal*, 12(4), 359–388. <https://doi.org/10.1007/s10040-004-0324-6>.
- Rahman, M. A. T. M. T., Majumder, R. K., Rahman, S. H., & Halim, M. A. (2011). Sources of deep groundwater salinity in the south western zone of Bangladesh. *Environmental Earth Sciences*, 63, 363–373. <https://doi.org/10.1007/s12665-010-0707-z>.
- Raymo, M. E., & Ruddiman, W. F. (1992). Tectonic forcing of late cenozoic climate. *Nature*, 359, 117–122. <https://doi.org/10.1038/359117a0>.
- Ronald Frost, B., & Carol Frost, D. (2008). A geochemical classification for feldspathic igneous rocks. *Journal of Petrology*, 49, 11. <https://doi.org/10.1093/petrology/egn/054>.
- Roy, S., Gaillardet, J., & Allegre, C. J. (1999). Geochemistry of dissolved and suspended loads of the Seine River, France: Anthropogenic impact, carbonate and silicate weathering. *Geochimica et Cosmochimica Acta*, 63(9), 1277–1292. [https://doi.org/10.1016/S0016-7037\(99\)00099-X](https://doi.org/10.1016/S0016-7037(99)00099-X).
- Safei, K., Arian, M.-A., & Mirhosseini, S. H. A. M. Z. (2015). Mineral chemistry and geothermometry of amphibole and plagioclase in the metabasites, located at the Tanbour Metamorphic Complex in Southern Iran. *Earth and Environmental Sciences*, 5(11), 795–808. <https://doi.org/10.4236/ojg.2015.511068>.
- Saravanan, K., Srinivasamoorthy, K., Gopinath, S., Prakash, R., & Suma, C. S. (2016). Investigation of hydrogeochemical processes and groundwater quality in Upper Vellar sub-basin Tamilnadu, India. *Arab Journal Geoscience*, 9, 372. <https://doi.org/10.1007/s12517-016-2369-y>.
- Sarin, M. M., Krishnaswami, S., Dilli, K., Somayajulu, B. L. K., & Moore, W. S. (1989). Major ion chemistry of the Ganga–Brahmaputra river system: Weathering processes and fluxes to the Bay of the Bengal. *Geochimica et Cosmochimica Acta*, 53(5), 997–1009. [https://doi.org/10.1016/0016-7037\(89\)90205-6](https://doi.org/10.1016/0016-7037(89)90205-6).
- Singh, S. K., Trivedi, J. R., Pande, K., Ramesh, R., & Krishnaswami, S. (1998). Chemical and Sr, O, C isotopic composition of carbonates from the Lesser Himalaya: Implications to the Sr isotopic composition of the source waters of Ganga, Ghaghara and Indus Rivers. *Geochimica et Cosmochimica Acta*, 62, 743–755.
- Soumya, B. S., Sekhar, M., Riotte, J. J., Audry, S., Lagane, C., & Braun, J. J. (2011). Inverse models to analyze the spatiotemporal variations of chemical weathering fluxes in a granito-gneissic watershed: Mule Hole, South India. *Geoderma*, 165(1), 12–24.
- Srinivas, Y., Muthuraj, D., Hudson Oliver, D., Stanley Raj, A., & Chandrasekar, N. (2013). Environmental applications of Geophysical and Geochemical methods to map groundwater quality at Tuticorin, Tamilnadu, India. *Journal of Environmental Earth Sciences*, 70(5), 2143–2152.

- Srinivasamoorthy, K., Chidambaram, S., Prasanna, M. V., Vasanthavigar, M., Peter, J., & Anandhan, P. (2008). Identification of major sources controlling groundwater chemistry from a hard rock terrain—A case study from Mettur taluk, Salem district, Tamil Nadu, India. *Journal of Earth System Science*, 117(1), 49–59. <https://doi.org/10.1007/s12040-008-0012-3>.
- Srinivasamoorthy, K., Gopinath, M., Chidambaram, S., Vasanthavigar, M., & Sarma, V. S. (2014). Hydrochemical characterization and quality appraisal of groundwater from Pungar sub basin, Tamil Nadu, India. *Journal of King Saud University-Science*, 26(1), 37–52. <https://doi.org/10.1016/j.jksus.2013.08.001>.
- Srinivasamoorthy, K., Nanthakumar, C., Vasanthavigar, M., Vijayaraghavan, K., Rajivgandhi, R., Chidambaram, S., Anandhan P., et al. (2009). Groundwater quality assessment from a hard rock terrain, Salem district of Tamilnadu, India. *Arabian Journal of Geosciences*, 4(1), 91–102. <https://doi.org/10.1007/s12517-009-0076-7>.
- Srinivasamoorthy, K., Vasanthavigar, M., Chidambaram, S., Anandhan, P., Manivannan, R., & Rajivgandhi, R. (2012). Hydrochemistry of groundwater from Sarabanga minor basin, Tamilnadu, India. *Proceedings of the International Academy of Ecology and Environmental Sciences*, 2(3), 193–203.
- Stallard, R. F., & Edmond, J. M. (1987). Geochemistry of the Amazon 3. Weathering chemistry and limits to dissolved inputs. *Journal of Geophysical Research: Oceans*, 92, 8293–8302. <https://doi.org/10.1029/JC092iC08p08293>.
- Stumm, W., & Morgan, J. J. (1996). *Aquatic chemistry: chemical equilibria and rates in natural waters* (3rd ed.). New York: Wiley.
- Sugavanam, E. B., Venkata Rao, V., Simhachalam, J., Nagal, S. C., & Sinha, A. K. (1976). Multiphase basic and ultrabasic activity in granulite terrain of North Arcot District, Tamil Nadu. *Journal of the Geological Society of India*, 17, 159.
- Talabi, A. O. (2015). Weathering of meta-igneous rocks in parts of the basement Terrain of South western Nigeria: Implications on groundwater occurrence. *International Journal of Scientific and Research*, 5(4), 17.
- Thangamani, S., & Raviraj, A. (2016). Rainfall variability and trend detection in Dindigul district of Amaravathi Basin. *Current World Environment*, 11(2), 567–576. <https://doi.org/10.12944/CWE.11.2.27>.
- Tipper, E. T., Lemarchand, E., Hindshaw, R. S., Reynolds, B. C., & Bourdon, B. (2012). Seasonal sensitivity of weathering processes: hints from magnesium isotopes in a glacial stream. *Chemical Geology*, 312–313, 80–92. <https://doi.org/10.1016/j.chemgeo.2012.04.002>.
- Toth, J. (1999). Groundwater as a geologic agent: An overview of the causes, processes, and manifestations. *Hydrogeology Journal*, 7, 1–14. <https://doi.org/10.1007/s100400050176>.
- Truesdell, A. H., & Jones, B. F. (1973). *WATEQ: A computer program for calculating chemical equilibria of natural waters*. U. S. Geological Survey, Report No. USGS-vIRD-73-007.
- Vyshnavi, S., & Islam, R. (2015). Water–rock interaction on the development of granite gneissic weathered profiles in Garhwal Lesser Himalaya, India. *Journal Earth System Science*, 124, 945–963. <https://doi.org/10.1007/s12040-015-0590-9>.
- Walker, J. C. G., Hays, P. B., & Kasting, J. F. (1981a). A negative feedback mechanism for the long-term stabilization of Earth's surface temperature. *Journal of Geophysical Research*, 86, 9776–9978.
- Walker, J. C. G., Hays, P. B., & Kasting, J. F. (1981b). A negative feedback mechanism for the long-term stabilization of Earth's surface temperature. *Journal of Geophysical Research*, 86(C10), 9776–9978.
- Wang, A., Xia, T., Ru, R., Yuan, J., Chen, X., & Yang, K. (2004). Antagonistic effect of selenium on oxidative stress, DNA damage, and apoptosis induced by fluoride in human hepatocytes. *Fluoride*, 37(2), 107–116.
- Wu, H., Zhang, J., & Ngo, H. H. (2015). A review on the sustainability of constructed wetlands for wastewater treatment: Design and operation. *Bioresource Technology*, 175, 594–601. <https://doi.org/10.1016/j.biortech.2014.10.06>.
- Yousef, A. F., Saleem, A. A., Baraka, A. M., & Aglan, O. (2009). The impact of geological setting on the groundwater occurrences in some Wadis in Shalatein–Abu-Ramad area, SE desert, Egypt. *European Water*, 25(26), 53–68.

Publisher's Note Springer Nature remains neutral with regard to jurisdictional claims in published maps and institutional affiliations.